

Structural and magnetic properties of $\text{Pr}_{1+x}\text{Ba}_{2-x}\text{Cu}_3\text{O}_{7+y}$

S. R. Hwang, W.-H. Li, and K. C. Lee

Department of Physics, National Central University, Chung-Li 32054, Taiwan, Republic of China

J. W. Lynn

NIST Center for Neutron Research, NIST, Gaithersburg, Maryland 20899

H. M. Luo and H. C. Ku

Department of Physics, National Tsing-Hua University, Hsinchu 300, Taiwan, Republic of China

(Received 30 October 2000; published 26 March 2001)

The effects of the incorporation of Pr atoms onto the Ba sites on the structural and magnetic properties of $\text{Pr}_{1+x}\text{Ba}_{2-x}\text{Cu}_3\text{O}_{7+y}$, with $x=0.22$ and 0.48 , were studied by using neutron diffraction and ac magnetic susceptibility measurements. Rietveld structural analysis shows that extra O atoms are pulled into the antichain sites, driving a structural change from an orthorhombic $Pmmm$ to a tetragonal $P4/mmm$ symmetry, when the chain and antichain sites become equally populated. Significant reductions in the ordering temperature of the Pr spins were found while the simple antiferromagnetic arrangement remained the same. These observations are consistent with the Pr-O distance increasing with increasing Pr doping. No changes in the structure or magnetic behavior were found for the CuO_2 layers.

DOI: 10.1103/PhysRevB.63.172401

PACS number(s): 75.25.+z, 61.12.-q, 75.50.Ee

The dramatic suppression of superconductivity and the high antiferromagnetic ordering temperature ($T_N=17$ K) of the Pr spins have made $\text{PrBa}_2\text{Cu}_3\text{O}_7$ a unique compound among the superconducting oxides $R\text{Ba}_2\text{Cu}_3\text{O}_{7-y}$ ($R123$, R is a rare earth).¹ Several mechanisms have been proposed to explain the singular behavior observed in Pr123 of which the one^{2,3} based on a strong hybridization between the Pr $4f$ orbital and the neighboring O $2p$ orbital in the CuO_2 layers is now believed to be the most significant. Recently, inhomogeneous superconductivity in Pr123 has been reported^{4,5} in systems where the c -axis lattice parameter is considerably longer than has usually been observed. Arguments for the appearance of superconductivity point in the direction that the substitution of Ba for Pr and the elongation of the Pr-O atomic distance may free, at least partially, the localized holes. In this paper, we present the results of structural and magnetic studies made, by means of neutron diffraction and ac magnetic susceptibility measurements, on two polycrystalline $\text{Pr}_{1+x}\text{Ba}_{2-x}\text{Cu}_3\text{O}_{7+y}$, with $x=0.22$ and 0.48 , where the Ba atoms were partially replaced by Pr atoms.

Two oxygenated polycrystalline samples were prepared using the standard solid-state reaction technique. Details of the preparation procedure can be found elsewhere.⁶ Structural analyses of the compounds were carried out using neutron-powder-diffraction measurements and Rietveld analysis.⁷ High-resolution neutron-powder-diffraction patterns taken at room temperature were collected on BT-1, the 32-detector-powder diffractometer at the National Institutes of Science and Technology (NIST) Center for Neutron Research. A Cu(311) monochromator crystal and a pyrolytic graphite (PG) filter were used to select a wavelength for the incident neutrons of $\lambda=1.5401$ Å. Angular collimations of $15'$, $20'$, and $7'$ full width at half maximum (FWHM) acceptance were employed for the in-pile, monochromatic, and diffracted beams, respectively.

It is well known that fully oxygenated $R123$ crystallizes into an orthorhombic $Pmmm$ symmetry. Replacing trivalent Pr atoms with divalent Ba atoms may tend to pull more O atoms into the system resulting in a structural change toward a tetragonal $P4/mmm$ symmetry due to the appearance of O atoms on the antichain sites. The General Structure Analysis System program⁸ was used to analyze the diffraction patterns for models assumed to belong to different symmetries but concentrated on the expected $Pmmm$ and $P4/mmm$ space groups. The results show that the $x=0.22$ and 0.48 compounds crystallize, respectively, into an orthorhombic $Pmmm$ symmetry and a tetragonal $P4/mmm$ symmetry. No mixing of the two structural phases was found in either compound. Figure 1 shows the observed (crosses) and fitted (solid lines) patterns for the $x=0.48$ compound, with their differences plotted at the bottom, indicating that they agree very well. The inset highlights one of the diffraction peaks that charac-

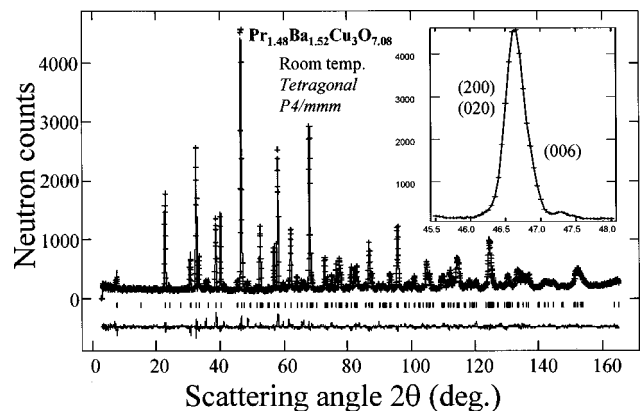


FIG. 1. Observed (crosses) and fitted (solid lines) high-resolution neutron powder diffraction patterns collected at room temperature for the $x=0.48$ compound. The inset shows the tetragonal fingerprint of the diffraction pattern.

TABLE I. Refined structural parameters for $\text{Pr}_{1+x}\text{Ba}_{2-x}\text{Cu}_3\text{O}_{7+y}$ where B represents the isotropic temperature parameter. The center of the unit cell is defined as at the Pr site, so that $\text{Pr}(\frac{1}{2}\frac{1}{2}\frac{1}{2})$, $\text{Ba/Pr}(\frac{1}{2}\frac{1}{2}z)$, $\text{O}(1)(xyz)$, $\text{Cu}(2)(00z)$, $\text{O}(2)(\frac{1}{2}0z)$, $\text{O}(3)(0\frac{1}{2}z)$, $\text{Cu}(1)(000)$, $\text{O}(4)(x\frac{1}{2}0)$, and $\text{O}(5)(\frac{1}{2}y0)$ show the orthorhombic symmetry. Setting $\text{O}(2)$ and $\text{O}(3)$ occupancies to be equivalent as well as $\text{O}(4)$ and $\text{O}(5)$ reduces the system to tetragonal symmetry.

		$x=0.22(2)$	$x=0.48(2)$
Space group		$Pmmm$	$P4/mmm$
a (Å)		3.8789(1)	3.8897(1)
b (Å)		3.9114(1)	3.8897(1)
c (Å)		11.6752(4)	11.6222(3)
Vol. (Å ³)		177.135	176.049
Pr	B (Å ²)	1.02(4)	1.02(3)
Ba/Pr	z	0.1795(1)	0.1787(2)
	B (Å ²)	1.09(3)	1.33(3)
	Frac.	0.89/0.11	0.76/0.24
O(1)	x	0.038(2)	0.038(2)
	y	0.036(2)	0.038(2)
	z	0.1591(1)	0.1598(2)
	B (Å ²)	1.11(1)	1.15(1)
	Frac.	1.00(2)	1.00(2)
Cu(2)	z	0.3494(1)	0.3494(1)
	B (Å ²)	0.67(4)	0.67(3)
O(2)	z	0.3725(2)	0.3691(1)
	B (Å ²)	0.98(1)	1.14(1)
O(3)	z	0.3728(2)	
	B (Å ²)	1.30(1)	
Cu(1)	B (Å ²)	1.37(5)	1.38(7)
O(4)	x	0.056(2)	0.071(2)
	B (Å ²)	1.48(3)	1.51(5)
	Frac.	0.82(2)	1.08(4)
O(5)	y	0.001(2)	
	B (Å ²)	1.53(5)	
	Frac.	0.18(2)	
O content		7.00(1)	7.08(1)
Pr-O(2) (Å)		2.4578(5)	2.4692(1)
Pr-O(3) (Å)		2.4427(5)	
Pr-O-Pr		105.280°	103.931°
χ		1.126	1.678

terizes the tetragonal symmetry where the coincident (200) and (020) peaks are plotted in an expanded scale. Allowing Ba to enter the Pr sites gives unacceptable poor fits for both compounds. Careful analyses of the occupancy factors give chemical formulas of $\text{Pr}(\text{Ba}_{0.89}\text{Pr}_{0.11})_2\text{Cu}_3\text{O}_{7.00}$ and $\text{Pr}(\text{Ba}_{0.70}\text{Pr}_{0.24})_2\text{Cu}_3\text{O}_{7.08}$ for the two compounds, which correspond to the 11% and 24% Pr-doped systems, respectively. No traces of any impurity phases, such as PrBaO_3 , PrCuO_3 , BaCuO_3 , and CuO_2 , were found, showing the samples were single phase. We estimated any impurity phase in the samples to be less than 2%. The refined structural parameters and the selected bond lengths for both the compounds are listed in Table I.

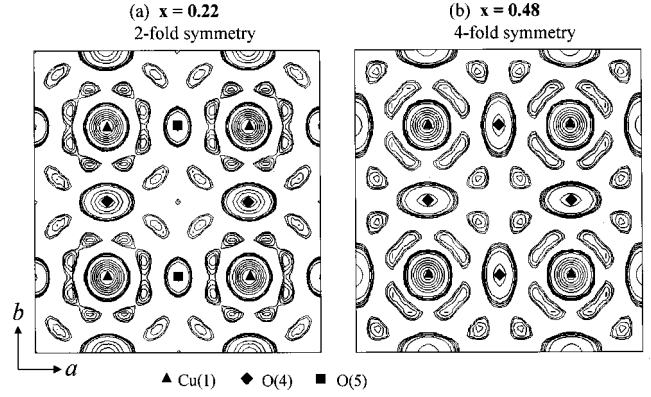


FIG. 2. Nuclear density contours of the CuO_{1+y} chain layer for the (a) $x=0.22$ and (b) $x=0.48$ compounds. Both maps cover $7.78 \text{ \AA} \times 7.78 \text{ \AA}$. The contours shown in (a) display a twofold symmetry whereas a fourfold symmetry is seen for those shown in (b).

Several features were seen and interpreted as trivalent Pr atoms incorporated onto the Ba sites. (1) The occupation of the antichain sites by O becomes feasible even in lightly doped compounds where the structure retains its orthorhombic $Pmmm$ symmetry. Unequal occupancy of the chain and anti-chain sites would preserve an orthorhombic symmetry as observed in the $x=0.22$ compound where 20% of O in the CuO chain layer was found to be located in the antichain sites. (2) Extra O atoms were incorporated into the CuO chain layers, which we believe is primarily to compensate for the additional charges due to Ba^{2+} being replaced by Pr^{3+} . For the $x=0.48$ compound, a structural change to tetragonal $P4/mmm$ symmetry was observed. This orthorhombic-to-tetragonal symmetry change can be clearly seen in the Fourier maps shown in Fig. 2 where the nuclear density contours of the CuO_{1+y} chain layers for both the compounds are displayed. The contours presented in Fig. 2(a) show a twofold symmetry whereas a fourfold symmetry may be seen in Fig. 2(b). (3) Similar to what has been observed in the isostructural La-doped⁶ and Nd-doped⁹ systems, the c axis in this Pr-doped system is shortened from the undoped case by nearly 1% for the $x=0.48$ compound. This is consistent with the smaller Pr atoms being used to replace the larger Ba atoms. More importantly, in the doped systems the average Pr-O separation increases noticeably and the Pr-O-Pr bond angle decreases. Compared to the undoped compound, the Pr-O(3) bond length increases by 1.4% while the Pr-O(2) bond length decreases by only 0.4% for the $x=0.48$ compound. This behavior is a direct consequence of the appearance of extra O atoms in the CuO_{1+y} chain layers, which pulls the neighboring (Ba/Pr)O and CuO_2 layers toward the CuO_{1+y} layers resulting in an increase in the separation between the Pr and CuO_2 layers.

The effects of Pr doping on the magnetic ordering of the Pr and Cu ions were studied by measuring the ac magnetic susceptibility and the magnetic neutron-diffraction patterns. The temperature dependence of the in-phase component of the ac susceptibility, $\chi'(T)$ was measured first to study the response of the system to a weak probing magnetic field. These measurements were performed using a conventional ac susceptometer. Neutron magnetic-diffraction patterns cov-

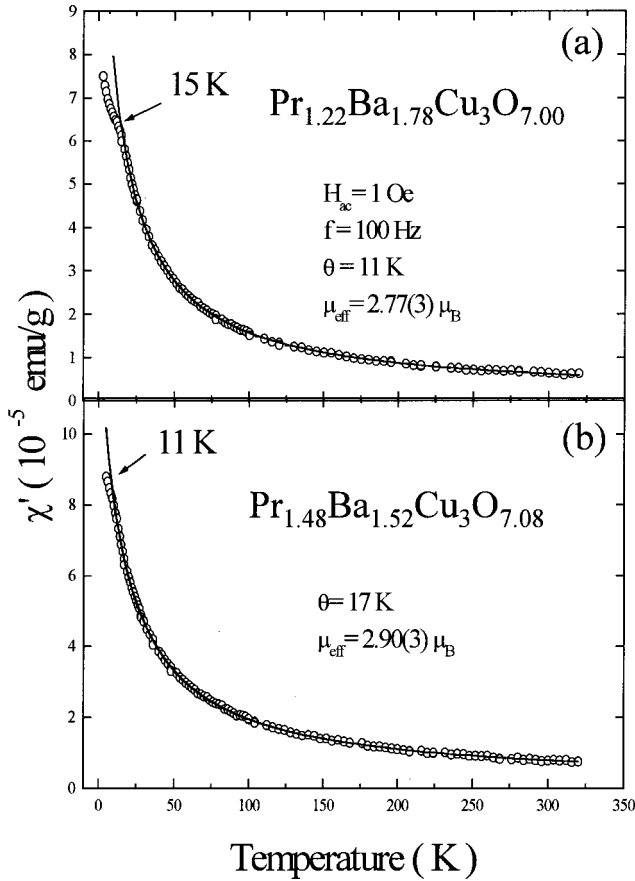


FIG. 3. Temperature dependence of the in-phase component of the ac susceptibility for the (a) $x=0.22$ and (b) $x=0.48$ compounds. Evidently $\chi'(T)$ departs from the Curie-Weiss behavior, shown as the solid curves, at low temperatures signaling the ordering of the Pr spins.

ering certain temperature regimes where the susceptibility showed anomalies were then collected to search for magnetic signals. The magnetic diffraction patterns were also collected at the NIST Center for Neutron Research using BT-2 triple-axis spectrometer with a PG(002) monochromator crystal to extract the $\lambda = 2.359 \text{ \AA}$ neutrons, PG filters, and $60' \cdot 40' \cdot 40'$ angular collimators.

It has been well accepted that the Pr spins in fully oxygenated Pr1237 orders antiferromagnetically below $T_N = 17 \text{ K}$.¹⁰⁻¹⁵ Shown in Figs. 3(a) and 3(b) are the $\chi'(T)$ for the $x=0.22$ and 0.48 compounds, respectively, measured using a weak probing field with an rms strength of 1 Oe and a frequency of 100 Hz. The $\chi'(T)$ observed for the present Pr-doped compounds has a similar behavior to the undoped system.¹⁶⁻¹⁸ The solid curves in Fig. 3 indicate the fits of data obtained between $25 \text{ K} < T < 200 \text{ K}$ to the Curie-Weiss expression for an antiferromagnetic system. Evidently, the fits depart from the Curie-Weiss expression at 15 and 11 K for the $x=0.22$ and 0.48 compounds, respectively, signaling the ordering of the Pr spins. Apparently, a lower ordering temperature is obtained for the more heavily doped compound, in agreement with previous results.¹⁵ These observations are closely related to the weakening of the superexchange coupling in Pr-O-Pr due to the elongation of the Pr-O

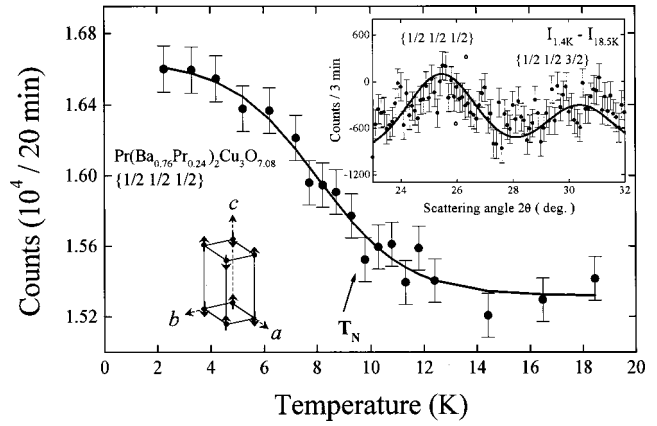


FIG. 4. Temperature dependence of the $\{1/2 1/2 1/2\}$ peak intensity for the $x=0.48$ compound showing a Neel temperature of $T_N \approx 11 \text{ K}$ for the Pr spins. The magnetic diffraction pattern obtained at 1.4 K and the proposed magnetic structure are shown in the insets.

bond and the narrowness of the Pr-O-Pr bond angle that is a result of Pr being incorporated onto the Ba sites. In addition, the effective moment was found to increase as values of $\mu_{\text{eff}}(\text{Pr}) = 2.77(3) \mu_B$ and $2.90(3) \mu_B$ were obtained for the $x=0.22$ and 0.48 compounds, respectively. As expected for antiferromagnetic systems, an applied dc magnetic field reduces the values for χ' in the ordered state while it has no obvious effect on χ' in the paramagnetic state.

The magnetic diffraction pattern for the $x=0.48$ compound, obtained at 1.4 K, is shown in the inset of Fig. 4 where the pattern taken at 18.5 K, serving as the nonmagnetic background, has been subtracted. Two resolution-limited magnetic peaks, which may be characterized by the $\{1/2 1/2 1/2\}$ wave vector, are clearly seen. They show a simple

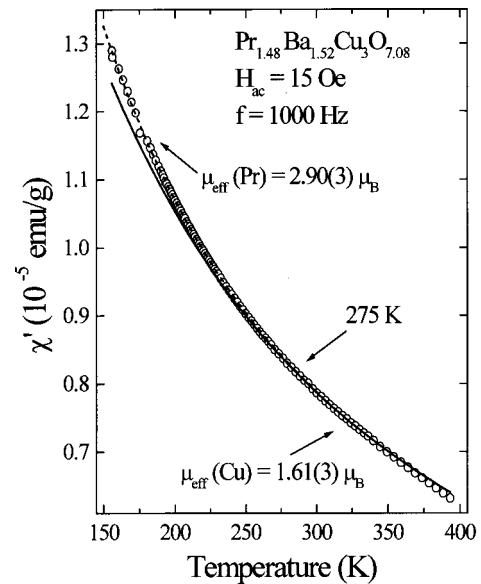


FIG. 5. $\chi'(T)$ of the $x=0.48$ compound, measured using a probing field with an rms strength of 15 Oe and a frequency of 10^3 Hz . The low- and high-temperature Curie-Weiss curves intersect at around 275 K signaling the ordering of the Cu spins.

antiferromagnetic order for the Pr spins as was observed for the undoped compound.¹⁰ The solid curves in the magnetic-diffraction pattern are the calculated curves assuming the same spin structure as that observed for the undoped system shown on the right in Fig. 4. A reasonably good agreement between the observed and calculated patterns is obtained. Plotted in Fig. 4 is the variation of the $\{\frac{1}{2}\frac{1}{2}\frac{1}{2}\}$ peak intensity with temperature, which reveals $T_N \approx 11$ K, determined to be at the inflection point of the curve for the Pr spins. This T_N , obtained from the neutron data, agrees well with that indicated by $\chi'(T)$. Apparently, there is no alteration in the spin structure but a reduction in T_N is observed in the Pr-doped systems.

Cu spins in undoped system have been observed^{19–23} to become ordered below 275 K. A close examination of the data in Fig. 3 reveals a small inflection at around 275 K. This inflection can be more readily seen in the $\chi'(T)$ that was measured using a stronger probing field. Shown in Fig. 5 is the $\chi'(T)$ for the $x=0.48$ compound, measured using a probing field with an rms strength of 15 Oe and a frequency of 10^3 Hz. The $\chi'(T)$ follows separate Curie-Weiss curves for temperatures above and below 275 K. Fitting the data obtained between 290 and 400 K to the Curie-Weiss expression gives the solid curve shown in the high temperature data in Fig. 5 whereas the dashed curve in the low-temperature data is the same curve shown in Fig. 3. The low- and high-

temperature curves meet at around 275 K, which signifies the ordering of the Cu spins as observed¹⁹ in the undoped system. Both the paramagnetic Pr and Cu spins then contribute to χ' at high temperatures. By assuming that these two components were statistically independent^{24,25} and using the paramagnetic parameters obtained at low temperatures for the Pr moment, we then obtained an effective moment of $\mu_{\text{eff}}(\text{Cu}) \approx 1.61(3)\mu_B$ for the Cu spins. Similar behavior and $\mu_{\text{eff}}(\text{Cu})$ values were obtained for the $x=0.22$ compound. No obvious effects on the Cu spin ordering were observed as Pr atoms were incorporated onto the Ba sites.

In conclusion, extra O atoms are pulled into the antichain sites when trivalent Pr atoms are used to replace divalent Ba atoms. A structural change, from an orthorhombic $Pmmm$ symmetry to a tetragonal $P4/mmm$ symmetry, occurs at sufficiently high doping. The appearance of the extra O in the chain layers pulls the neighboring (Ba/Pr)O and CuO_2 layers slightly towards them resulting in a larger separation between the Pr-O atoms, hence a weaker superexchange coupling for Pr-O-Pr. Consequently, the T_N of Pr is reduced while the spin structure remains a simple antiferromagnetic arrangement. No significant structural or magnetic alterations in the CuO_2 layers were found.

This work was supported by the National Science Council of the R.O.C. under Grants Nos. NSC 89-2112-M-008-051 (NCU) and NSC 89-2112-M-007-023 (NTHU).

-
- ¹For a review, see H. B. Radousky, *J. Mater. Res.* **7**, 1917 (1992).
²Y. Takano, S. Yokoyama, K. Kanno, and K. Sekizawa, *Physica C* **252**, 61 (1995).
³J. W. Lynn, N. Rosov, S. N. Barilo, L. Kurnevitch, and A. Zhokhov, *Chin. J. Phys. (Taipei)* **38**, 286 (2000).
⁴H. A. Blackstead, J. D. Dow, D. B. Chrissy, J. S. Horwitz, M. A. Black, P. J. McGinn, A. E. Klunzinger, and D. B. Pulling, *Phys. Rev. B* **54**, 6122 (1996).
⁵Z. Zou, J. Ye, K. Oka, and Y. Nishihara, *Phys. Rev. Lett.* **80**, 1074 (1998).
⁶H. Y. Wang, S. R. Hwang, W.-H. Li, K. C. Lee, J. W. Lynn, H. M. Luo, and H. C. Ku, *Phys. Rev. B* (to be published).
⁷H. M. Rietveld, *J. Crystallogr.* **2**, 65 (1969).
⁸A. C. Larson and R. B. Dreele, Los Alamos National Laboratory Report No. LA-UR-86-748, 1990 (unpublished).
⁹M. J. Kramer, K. W. Dennis, D. Falzgraf, R. W. McCallum, S. K. Malik, and W. B. Yelon, *Phys. Rev. B* **56**, 5512 (1997).
¹⁰W.-H. Li, J. W. Lynn, S. Skanthakumar, T. W. Clinton, A. Kebede, C.-S. Jee, J. E. Crow, and T. Mihalsin, *Phys. Rev. B* **40**, 5300 (1989).
¹¹S. Skanthakumar, J. W. Lynn, N. Rosov, G. Cao, and J. E. Crow, *Phys. Rev. B* **55**, R3406 (1997).
¹²S. Uma, W. Schnelle, E. Gmelin, G. Rangarajan, S. Skanthakumar, J. W. Lynn, R. Walter, T. Lorenz, B. Bücher, and A. Erb, *J. Phys. (Lett.)* **10**, L33 (1998).
¹³A. T. Boothroyd, A. Longmore, N. H. Andersen, E. Brecht, and Th. Wolf, *Phys. Rev. Lett.* **78**, 130 (1997).
¹⁴J. P. Hill, A. T. Boothroyd, N. H. Andersen, E. Brecht, and Th. Wolf, *Phys. Rev. B* **58**, 11 211 (1998).
¹⁵For a review, see J. W. Lynn, *J. Alloys Compd.* **250**, 552 (1997).
¹⁶D. B. Mitzi, P. T. Feffer, J. M. Newsaw, K. J. Webb, P. Klavins, A. J. Jacobson, and A. Kapitulnik, *Phys. Rev. B* **38**, 6667 (1998).
¹⁷B. Okai, M. Kosuge, H. Nozaki, K. Takahashi, and M. Ohta, *Jpn. J. Appl. Phys., Part 2* **27**, L41 (1988).
¹⁸L. Soderholm and G. L. Goodman, *J. Solid State Chem.* **81**, 121 (1989).
¹⁹For a recent review, see J. W. Lynn and S. Skanthakumar, in *Handbook on the Physics and Chemistry of Rare Earths*, edited by K. A. Gschneidner, Jr., L. Eyring, and M. B. Maple (North-Holland, Amsterdam, in press), Vol. 31, Chap. 198.
²⁰S. K. Malik, S. M. Pattalwar, C. V. Tomy, R. Prasad, N. C. Soni, and K. Adhikary, *Phys. Rev. B* **46**, 524 (1992).
²¹S. K. Malik, R. Prasad, N. C. Soni, K. Adhikary, and W. B. Yelon, *Physica B* **224**, 562 (1996).
²²V. N. Narozhnyi, D. Eckert, K. A. Nenkov, G. Fuchs, T. G. Uvarova, and K.-H. Müller, *Physica C* **312**, 233 (1999).
²³A. T. Boothroyd, A. Longmore, N. H. Andersen, E. Brecht, and Th. Wolf, *Phys. Rev. Lett.* **78**, 130 (1997).
²⁴J. S. Smart, *Effective Field Theories of Magnetism* (Saunders, London, 1966).
²⁵M. Tovar, *J. Appl. Phys.* **83**, 7201 (1998).